Kinetic and Mechanistic Studies of the Reaction of Hydroxyl Radicals with Acetaldehyde over an Extended Temperature Range

Philip H. Taylor[$#], M. Sm. Rahman[#], M. Arif[#], B. Dellinger[#], and P. Marshall[%]

[$]Corresponding Author
[#]Environmental Sciences and Engineering Group
University of Dayton Research Institute
300 College Park
Dayton, OH 45469-0132
(513) 229-3604
FAX (513) 229-2503
Internet: Taylorph@udri.udayton.edu

[%]Department of Chemistry
University of North Texas
P. O. Box 5068
Denton, TX 76203
(817) 565-2294
FAX (817) 565-4318
Internet: Marshall@unt.edu

Submitted for Presentation at the Twenty-Sixth International Symposium on Combustion

Preference: Oral Presentation

Colloquium Topic: General Reaction Kinetics or NO_X, SO_X and Pollutant Emission Kinetics

Word Count: 4200 via MS Word 5.1a
4 Figures and 1 Regular Size Table: 1000 Words
1 Small Table: 100 Words
2 equations embedded in text: ~100 words

Total: 5400 words

Abstract

Absolute rate coefficients for the reactions of OH with CH_3CHO, CH_3CDO, and CD_3CDO were measured with the laser photolysis/laser-induced fluorescence technique. A large majority of the kinetic data were obtained at 740 torr of helium pressure over the temperature range 295-900 K. Measurements below 600 K exhibited a negative temperature dependence while measurements above 600 K exhibited a positive temperature dependence. CH_3CHO + OH measurements at 100, 300, 400, and 740 torr helium pressure indicated the lack of a pressure dependence. Possible reaction pathways were evaluated with a quantum RRK model incorporating nonempirical electronic structure calculations on the reactants and transition-state structures. Two different reaction mechanisms were shown to dominate, depending on the temperature. A mechanism involving OH addition followed by CH_3 elimination was dominant at low temperatures. A mechanism involving H-atom abstraction from the $-CH_3$ group was dominant at elevated temperatures. Evidence is also presented for H-atom abstraction from the ketyl (CHO) group at low temperatures. Kinetic isotope effect measurements using CH_3CDO and CD_3CDO support the proposed mechanisms.

Introduction

Acetaldehyde (CH_3CHO), a hazardous air pollutant regulated under Title III of the Clean Air Act Amendments, is known for its photochemical reactivity in the atmosphere.[1] CH_3CHO quickly reacts under atmospheric conditions to produce peroxyacetyl nitrate (PAN), a strong eye irritant which is phytotoxic and has been linked with mutagenic activity and possible skin cancer.[2,3] CH_3CHO is known to be emitted from internal conbustion engines fueled with either gasoline or alternative automotive fuels including M85, E85, natural gas, LP gas, and reformulated gasoline.[4-6]

The reaction of hydroxyl (OH) radical with CH_3CHO is important under both atmospheric and combustion conditions. Previous experimental measurements have been limited to relatively low temperatures (<550 K) and have been conducted largely to understand the mechanism of oxidation of CH_3CHO under atmospheric conditions. The mechanism of reaction under atmospheric and higher temperature conditions characteristic of combustion remains poorly understood due to the lack of definitive product and mechanistic data.

Atkinson and Lloyd[7] reported the formation of PAN from the room temperature reaction of OH with CH_3CHO in air in the presence of NO_x. They reported that the following mechanism involving H-atom abstraction was consistent with their observations:

$$OH + CH_3CHO \text{ ---> } H_2O + CH_3CO$$

$$CH_3CO + O_2 \text{ ---> } CH_3C(O)OO$$

$$CH_3C(O)OO + NO_2 \text{ ---> } CH_3C(O)OONO_2 \text{ (PAN).}$$

Because this mechanism involves abstraction of the sole ketyl (CHO) hydrogen, it is consistent with the observation that the room temperature rate coefficients for the $\geq C_2$ aldehydes are reasonably similar, increasing only slightly with the length of the alkyl side chain and showing that the alkyl substituent has only a minimal effect on the OH radical rate coefficient. They also proposed that the negative temperature dependence of the OH rate constant reported by several researchers[8] (cf. Fig. 1) indicates that although the reaction proceeds by overall H-atom

abstraction, the reaction involves initial OH radical addition followed by rapid decomposition of the adduct to the observed products.

This manuscript presents absolute rate coefficient measurements for the following reaction

$OH + CH_3CHO$ -----> products (1)

over an extended temperature range using a laser photolysis/laser-induced fluorescence technique. At selected temperatures, the effect of total pressure on the $OH + CH_3CHO$ rate constant has also been evaluated. The results were analyzed using a Quantum RRK model[9] describing the competition between chemically activated OH addition and H-atom abstraction mechanisms. Hartree Fock *ab initio* calculations were used to define the activated complex for H-atom abstraction from the $-CH_3$ group and the multiple decomposition channels of the chemically activated adduct. The experimental results are consistent with a mixture of chemically activated OH addition/CH_3 elimination and H abstraction from the ketyl group at low temperatures and H-atom abstraction from the $-CH_3$ group at elevated temperatures. Kinetic isotope effect measurements using CH_3CDO and CD_3CDO over an extended temperature range support this mechanism.

Experimental Approach and Data Reduction

The experimental procedures were very similar to previous studies of OH reactions with chlorinated hydrocarbons[10-12] and hydrochlorofluorcarbons.[13] As a result, we only briefly summarize the procedures here.

OH radicals were produced by 193.3 nm photodissociation of $CH_3CHO/N_2O/H_2O$/He gas mixtures with a ArF excimer laser (Questek Model 2860). Initial OH concentrations, $[OH]_0$, ranged from 2×10^{10} to 4×10^{10} molecules cm^{-3} and were determined from published values of the N_2O absorption coefficient (8.95×10^{-20} cm^2 $molecule^{-1}$ at 298 K),[14] a photodissociation quantum yield for $O(^1D)$ production of unity,[15] and the rapid reaction of $O(^1D)$ with H_2O (95% conversion in < 20 μs). Experiments were conducted for photolysis laser intensities of 1 to 2 mJ cm^{-2}. Following reaction initiation, time-resolved OH profiles were measured as functions of reactant concentration using laser-induced fluorescence with a pulsed Nd:YAG pumped dye laser (Quanta

Ray Model DCR-2/PDL-2) emitting at the wavelength of 282.1 nm. Broadband fluorescence was collected at 309 nm using a PMT/bandpass filter combination.

In order to control the temperature uniformly, four symmetrical ceramic heaters surround the optical reactor adjacent to the reaction zone. The gas temperature was measured with a chromel-alumel thermocouple positioned ~2 mm from the probe intersection volume. Measurements using a second retractable chromel-alumel thermocouple indicated a variation of less than 3 K across the detection volume for gas temperatures ranging from 295 K to 1000 K. All experiments were carried out under slow flow conditions and the buildup of reaction products was minimized. Individually controlled gas flows of $CH_3CHO/N_2O/H_2O$/He were thoroughly mixed before entering the optical reactor. The composite flow conditioned the reactor for 1-3 minutes prior to the onset of data collection, thereby minimizing any effects due to reactant adsorption on the reactor walls. A majority of the experiments were conducted at a total pressure of 740±10 torr. Some additional experiments were conducted at pressures of 100, 300, and 400 torr. Pressures were measured with a calibrated vacuum gauge. Flow rates were controlled with differential flow transducers and were checked following each experiment using the soap bubble technique. To provide additional information on the mechanism, measurements for CH_3CDO and CD_3CDO were also obtained over an extended range of temperatures at a pressure of 740 torr helium.

For all experiments, reactive and diffusive OH radical decay profiles exhibited exponential behavior and were fitted by the following nonlinear expression

$$[OH] = [OH]_0 \exp(-k't) + \gamma,$$

where γ is the constant background signal level and t is the time delay between the two lasers. Because $[CH_3CHO] > 1000[OH]$ in all reactive experiments, exponential OH radical decays, of pseudo-first-order decay constant $k' = k[CH_3CHO] + k_d$, were observed. k_d is the first order rate constant for OH radical disappearance from the probe volume due to diffusion and reaction with impurities in the carrier gas. The bimolecular rate constant, k, was obtained from the slope of the least-squares straight line through the graph of k' versus $[CH_3CHO]$.

Stock samples of CH_3CHO, CH_3CDO, and CD_3CDO were obtained from Aldrich, Inc. Gas chromatography-mass spectrometry (GC/MS) analyses indicated the stock samples were free of contaminants (>99.9% pure). The remaining chemicals used in our gas delivery system had the following stated minimum purities: He (99.999+%); N_2O (99.9%); H_2O (HPLC organic-free reagent grade). Absorption cross sections for the reactants were very small (on the order of 10^{-21} cm^2 $molecule^{-1}$)[16] in comparison with N_2O at 193 nm. Thus, laser photolysis of the reactants was expected to be insignificant. This was verified by numerous experiments where variation of the excimer laser intensity had no observable effect on OH decays.

Results

Absolute rate measurements for the reaction of OH with CH_3CHO were obtained from 295 to 900 K. 2σ error limits, based on a propagation of error analysis, ranged from ±8% to ±27%. The experimental results, along with previous measurements[17-23], are presented in Arrhenius form in Fig. 1. A negative temperature dependence was observed for the experimental measurements between 295 and 600 K. This result was consistent with previous measurements.[17,22,23] The rate coefficients determined from these measurements were approximately 22% smaller than Atkinson's recommendation[8] based on previous measurements. This difference is within the combined uncertainties of the various experimental techniques (typically about ±20%).

Figure 1

Prior to this study, there were no measurements reported above 538 K. Above 600 K, our measurements indicate a change in temperature dependence from negative to positive. Above 900 K, experimental measurements were not possible due to thermal decomposition of the sample. The experimental results for the two apparently different mechanisms of reaction were well represented by the following simple Arrhenius expressions:

$$k_{295\text{-}550\ K} = (4.31\pm0.22) \times 10^{-12} \exp[(309\pm19)/T \quad cm^3/molecule\text{-}s$$

$$k_{600\text{-}900\ K} = (1.89\pm0.26) \times 10^{-11} \exp[(-597\pm108)/T \quad cm^3/molecule\text{-}s.$$

where error limits represent $\pm2\sigma$ (95% confidence intervals).

Discussion

The negative temperature dependence of $k_1(T)$ is well established by the present and the earlier work.[17,22,23] This observation mmediately suggests the possibility of an addition-elimination mode for reaction (1) at low temperatures (<600 K), e.g.

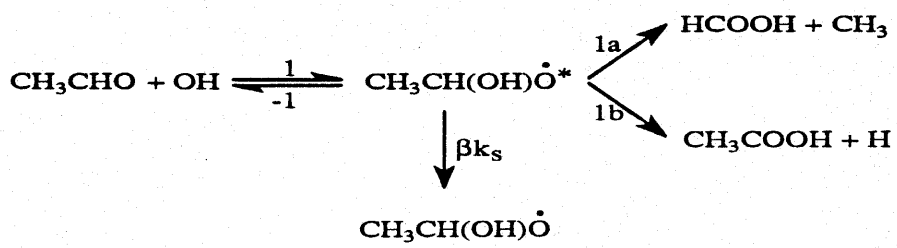

since many addition reactions of OH show overall negative temperature dependence at these temperatures.[8] Reaction (1) would undoubtedly proceed through a vibrationally excited adduct that would be expected to undergo collisional stabilization βk_S in addition to forward (k_{1a} or k_{1b}) and reverse (k_{-1}) decompositions. A pathway analogous to rxn (1b) has already been suggested in the related formaldehyde (HCHO) case.[24]

To examine the possibility of OH addition, we have obtained rate measurements at 100, 300, and 400 torr, in addition to our atmospheric pressure measurements, at temperatures of 295 and 600 K. The results, presented in Fig. 1, indicate there is no pressure dependence for reaction (1). The good agreement between the low pressure DF-RF results[17] and the higher pressure FP-RF results[22] are consistent with our experimental observations. Hence, if the adduct path exists then either the adduct is always stabilized and reaction (1) is in the high pressure limit above 1.5 torr helium, or the forward dissociation paths to either acetic acid and H atoms or formic acid and methyl radicals is much faster than the average dissociation path back to reactants. Michael et al.[17] ruled out the reaction (1b) on the basis of H atom scavenger experiments using NO_2. However, they could not rule out reaction (1a). Nonetheless, they noted that the overall exothermicity to CH_3 + HCOOH was only 3.8 kcal/mol lower than that to H + CH_3COOH (-26.2 and -22.4 kcal/mol, respectively[25]). Thus, one might anticipate the significance of one pathway may imply significance for the other, particularly at higher temperatures. This is of course not a firm

conclusion since models for the transition states associated with the two pathways must be carefully considered (*vide infra*).

A completely different alternative to the displacement reactions just considered is the direct metathetical abstraction process that would appear consistent with the positive temperature dependent rate data observed above 600 K:

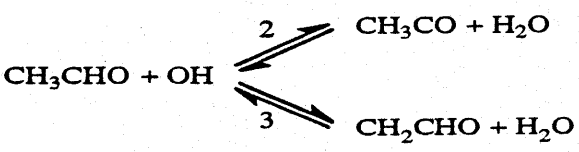

Reaction (2) is considered to be more likely because the ketyl H-atom bond strength is much lower than that for methyl (86.4 compared to ~98 kcal/mol, respectively). Indeed, acetyl (CH_3CO) radicals were the only observed radicals in the related Cl-atom abstraction reaction.[26]

The two alternatives then suggest that either stabilized adduct radicals, HCOOH + CH_3 formation, or acetyl radicals are the most probable products of reaction (1). To examine carefully the possibilities of chemically activated OH addition versus H-atom abstraction, Quantum RRK calculations were carried out for reaction (1) using *ab initio* modeling and thermochemical transition state theory (TST) calculations of the critical high pressure limit rate parameters.

QRRK Input Calculations

To obtain the necessary information about the potential energy surface *ab initio* calculations[27] were carried out implemented with the Gaussian 92 program.[28] Hartree-Fock calculations with the 6-31G(d) basis set identified geometries and frequencies for the reactants, the stabilized CH_3CHO + OH adduct, the products of H-atom abstraction reactions and the adduct decomposition reactions, and the transition states that connect these species. These HF/6-31G(d) geometries were then refined with a partial correction for the effects of electron correlation at the MP2/6-31G(d) level of theory. Much higher level single-point Gaussian-2 and G2(MP2) calculations[29] provided relative energies (corrected to 298 K) for each stable species and the transition states.

Figure 2

A potential energy diagram for the addition/elimination channels is presented in Fig. 2. Heats of formation for OH, CH_3, H, H_2O, HCOOH, CH_3COOH, and CH_3CHO were taken from Wagman et al.[25] The heat of formation for the adduct was calculated using $CH_3CH(OH)_2$ as a model compound based on an O-H bond dissociation energy of 104.2 kcal/mol. A similar value (within 2 kcal/mol) was obtained from our *ab initio* calculations. The adduct is bound by ~20 kcal/mol relative to the reactants. The adduct decomposition channels (CH_3COOH + H and HCOOH + CH_3) were found to be approximately 1.0 and 5.5 kcal/mol lower lying in energy compared to the stabilized adduct.

Table 1

Quantum RRK input parameters are summarized in Table 1. A saddle-point could not be identified for the OH addition reaction, k_1. High-pressure limit rate parameters for OH addition to CH_3CHO were therefore selected to be approximately equal to the recommended value for C_2H_4 + OH (9.0×10^{-12} $(T/298)^{-1.1}$ cm^3 $molecule^{-1}$ s^{-1}).[8] A zero exponential term is consistent with the lack of an *ab initio* energy barrier. The reverse decomposition of the stabilized adduct to reactants was calculated by detailed balancing. High-pressure limit adduct decomposition channels (k_{1a} and k_{1b}) were calculated using thermochemical TST procedures and the *ab initio* HF/6-31G(d) geometries and frequencies. A larger gain in entropy of activation was observed for the HCOOH + CH_3 channel, resulting in a larger A factor. The Arrhenius coefficients reported in Table 1 were derived from rate coefficients calculated between 295 to 1000 K. The activation energies for these channels were determined using the following relation $E_a = \Delta H_r + E_{arev}$. On the basis of experimental measurements for H-atom and CH_3 radical addition to olefins,[31] E_{arev} was set equal to 2.0 for the H elimination channel and 7.0 for the CH_3 elimination channel.

An analysis of the relative energies of the H-atom abstraction products indicated that H-atom abstraction from the ketyl-H atom was clearly the dominant of the two pathways. *Ab initio* studies of H-atom abstraction from the ketyl group resulted in a potential energy surface very different from that observed for the more conventional H-atom abstraction from the -CH_3 group. Clear saddlepoints were derived from HF/6-31G(d) and MP2/6-31G(d) calculations, but G2(MP2) and G2 energies at these geometries lay significantly below the reagents. QCISD(T)/6-311G(d,p)

energies at selected points along the MP2/6-31G(d) reaction coordinate revealed a very loose transition state with a barrier of less than 1 kcal mol^{-1}, which decreases when changes in zero-point energy are included. Thus, the potential energy surface was flat and had character more typically ascribed to an addition-type reaction. As a result, thermochemical TST calculation of the rate coefficient parameters could not be carried out. Instead, we have utilized experimental data for the OH + HCHO reaction[8] to describe this channel. This reaction has been shown to occur by H-atom abstraction at room temperature.[32] Rate measurements between ~200 and 500 K have indicated a negligible or slightly negative temperature dependence. Atkinson[8] has recommended the following rate expression which fits the available data from ~200 to 500 K and is in agreement with much higher flame-derived rate coefficients (in units of cm^3/molecule-s):

$$k = 1.25 \times 10^{-17} T^2 \exp(1287/RT).$$

Correcting largely for reaction path degeneracy, we have used this expression to derive an expression for H-atom abstraction from the ketyl group (cf. Table 1).

Thermochemical TST calculations were carried out for the slower H-atom abstraction from the CH_3 group. The transition state geometry and frequencies for H-atom abstraction from the $-CH_3$ group are presented in Fig. 3. The temperature dependence of the pre-exponential factor was evaluated using a procedure developed by Cohen.[33] Calculations were carried out assuming both free internal rotations and hindered internal rotations for the two new internal rotors created in the activated complex. For the hindered internal rotations, the barriers to rotation were calculated using scaled *ab initio* frequencies. The harmonic modes which most closely corresponded to $CH_3COH\cdots OH$ and $CH_3CO\cdots HOH$ internal rotations were identified by visualization of the normal modes.[34] A value for the exponential term for H-atom abstraction from the $-CH_3$ group of 1.0 kcal/mol was selected to complete these calculations, based on the same experimental value derived from $OH + C_2H_6$.[35]

The remaining Quantum RRK input parameters included molecular parameters for He bath gas and the adduct and the geometric mean frequency for the adduct. The Lennard-Jones parameters, σ and ϵ, for He and were obtained from Kee et al.[36] Similarly, σ and ϵ for the adduct

were calculated using relations from kinetic gas theory based on values for CH_3CHO and OH from Kee et al.[36] The geometric mean frequency for the adduct was calculated from frequencies given by the *ab initio* calculations.

QRRK Calculations

The results of the QRRK calculations at 740 torr helium pressure are shown in Fig. 4. Rate coefficients for H-atom elimination, CH_3 elimination, H-atom abstraction from the ketyl group, and H-atom abstraction from the -CH_3 group are shown along with the sum of these channels and the experimental measurements. The agreement between the measured and calculated total rate coefficient is very good. The rate coefficient for stabilization of the adduct is much smaller in magnitude than the other reaction channels and is not shown.

The QRRK calculation demonstrated a complex coupling of four reaction channels as a function of temperature: OH addition/CH_3 elimination, OH addition/H-atom elimination, H-atom abstraction from the ketyl group, and H-atom abstraction from the -CH_3 group. The calculations indicated that CH_3 elimination dominated the observed rate measurements between 295 and 400 K. At 295 K, CH_3 elimination, H-atom elimination, and H-atom abstraction from the ketyl group accounted for 74%, 17%, and 8% of the observed rate, respectively. At ~500 K, the contributions from both H-atom abstraction channels increased and became roughly equal to the contribution from the H-atom elimination channel (~13%). Above 500 K,the dominant reaction channels were CH_3 elimination and H-atom abstraction from both the ketyl group and the -CH_3 group. Above 750 K, H-atom abstraction from the -CH_3 became the dominant reaction channel. At 900 K, the relative contributions of H-atom abstraction from the -CH_3 group, CH_3 elimination, and H-atom abstraction from the CHO group were 55%, 28% and 17% of the observed rate.

QRRK calculations indicated that the significant reaction channels (all except adduct stabilization) were independent of total pressure. This result is consistent with experimental measurements.

To determine whether the mechanistic implications of the QRRK calculations described were plausible, we carried out additional rate coefficient measurements using deuterated and

perdeuterated reactants. The measured rate coefficients for CH_3CDO and CD_3CDO, obtained at 740 torr total helium pressure, at temperatures of 295, 400, 600, and 750 K are presented in Table 2. Also given in Table 2 are the respective kinetic isotope ratios, k_{CH3CHO}/k_{CH3CDO} and k_{CH3CHO}/k_{CD3CDO}. Measurable kinetic isotope effects were observed for CH_3CDO at room temperature and for CD_3CDO at all four temperatures. Of particular significance was the observed kinetic isotope effect for CH_3CDO at room temperature, indicating that H-atom abstraction from the ketyl group does occur. This result also supports the findings of the *ab initio* calculations suggesting the lack of an appreciable barrier to this reaction. At elevated temperatures, the observed kinetic isotope effect for CD_3CDO is consistent with model predictions regarding the increased importance of H-abstraction from $-CH_3$ at elevated temperatures.

In summary, the reported measurements and QRRK analysis of the CH_3CHO + OH reaction indicate that OH addition followed by CH_3 elimination is the dominant reaction pathway at temperatures between 295 and 600 K. The deuterated isotope studies support the previous contention of Atkinson and Lloyd[7] that H-atom abstraction from the ketyl group does occur at temperatures pertinent to atmospheric conditions. However, our QRRK calculations suggest that this is a minor pathway. Our calculations also support the findings of Michael, et al.[17], i.e., the H-atom elimination pathway is largely insignificant, except possibly at the lowest temperatures. The dominant reaction channel at combustion temperatures is postulated to be H-atom abstraction from the methyl group. The branching ratios for the various reaction channels derived from the QRRK calculations must be considered with caution due primarily to the uncertainty in the estimated rate parameters for k_2. Variational transition state theory analysis[37] of k_2 is necessary to quantify this unusual H-atom abstraction reaction more carefully.

Acknowledgments

PT, SR, MA and BD acknowledge support from the Environmental Protection Agency (Grant R819861-01-0). PM thanks the Wright Laboratory for a generous grant of computer time and the R. A. Welch Foundation (Grant B-1174) for support.

References

1. Kao, A.S., *J. Air & Waste Manage. Assoc.* 44: 683-696 (1994).

2. Kleindiest, T.E., Shepson, P.B., Smith, D.F., Hudgens, E.E., Nero, C.M., Cupitt, L.T., Bufini, J.J., Claxton, L.D., *Environ. Molecular Mutagen* 16: 70-80 (1990).

3. Shepson, P.B., Kleindiest, T.E., Edney, E.O., Nero, C.M., Cupitt, L.T., and Claxton, L.D., *Environ. Sci. Technol.* 20: 1008-1013 (1986).

4. California Air Resources Board, *Proposed Reactivity Adjustment Factors for Transitional Low-Emissions Vehicles-Staff Report and Technical Support Document*, Mobile Sources Division, El Monte, CA. 1991.

5. California Air Resources Board, *Preliminary Reactivity Adjustment Factors*, Mobile Sources Division, El Monte, CA. 1994.

6. Taylor, P.H., Shanbhag, S., and Dellinger, B., in *Progress in Emission Control Technologies (SP-1053)*, SAE Technical Paper Series, Warrendale, PA, 1994, #941904, p. 39-49.

7. Atkinson, R. and Lloyd, A.C., *J. Phys. Chem. Ref. Data* 13: 315-444 (1984).

8. Atkinson, R., *J. Phys. Chem. Ref. Data* Monograph 1 (1989).

9. Dean, A.M., *J. Phys. Chem.* 89: 4600-4608 (1985).

10. Jiang, Z., Dellinger, B., and Taylor, P.H., *J. Phys. Chem.* 96: 8961-8964 (1992).

11. Jiang, Z., Dellinger, B., and Taylor, P.H., *Int. J. Chem. Kinet.* 25: 9-23 (1993).

12. Jiang, Z., Taylor, P.H., and Dellinger, B., *J. Phys. Chem.* 97: 5050-5053 (1993).

13. Fang, T.D., Taylor, P.H., and Dellinger, B., accepted, *J. Phys. Chem.* 1995.

14. Selwyb, G., Podolske, J., Johnston, H. S., *Geophys. Res. Lett.* 4: 427-430 (1977).

15. Simonaitis, R., and Heicklen, J., *J. Phys. Chem.* 77: 1932-1935 (1973).

16. Lake, J.S. and Harrison, A.J., *J. Chem. Phys.* 30: 361 (1959). Calvert, J.G. and Pitts, J.N., Jr., *Photochemistry*, 2nd ed., John Wiley: New York, 1967).

17. Michael, J.V., Keil, D.G., and Klemm, R.B., *J.Chem.Phys.* 83: 1630-1636 (1985).

18. Morris, Jr., E.D., Stedman. D.H., and Niki, H.,*J.Amer. Chem.Soc.* 93: 3570 (1971).

19. Morris, Jr., E.D. and Niki, H. *J. Phys. Chem.* 75: 3640-3641 (1971).

20. Niki, H., Maker, P.D., Savage, C.M., and Breitenbach, L.P., *J. Phys. Chem.* 82: 132-134 (1978).

21. Kerr, J.A. and Sheppard, D.W., *Environ. Sci. Technol.* 15: 960-963 (1981).

22. Atkinson, R. and Pitts Jr., J.N., *J. Chem.Phys.* 68: 3581-3584 (1978).

23. Semmes, D.H., Ravishankara, A.R., Gump-Perkins, C.A., and Wine, P.H., *Int. J.Chem.Kinet.* 17: 303-313 (1985).

24. Horowitz, A., Su, F., and Calvert, J.G., *Int. J. Chem. Kinet.* 10: 1099 (1978).

25. Wagman, D.D., Evans, W. H., Parker, V. B., Schumm, R. H., Halow, I., Bailey, S. M., Churney, K. L., Nuttall, R. L. *J. Phys. Chem. Ref. Data* 11: Supplement 2 (1982).

26. Slagle, I.R. and Gutman, D., *J. Am. Chem. Soc.* 104: 4741 (1982).

27. Hehre, W. J., Radom, L., Schleyer, P. v. R., Pople, J. A. *Ab Initio Molecular Orbital Theory*; Wiley: New York, 1986.

28. Frisch, M. J.; Trucks, G. W.; Head-Gordon, M.; Gill, P. M. W.; Wong, M. W.; Foresman, J. B.; Johnson, B. G.; Schlegel, H. B.; Robb, M. A.; Replogle, E. S.; Gomperts, R.; Andres, J. L.; Raghavachari, K.; Binkley, J. S.; Gonzalez, C.; Martin, R. L.; Fox, D. J.; DeFrees, D. J.; Baker, J.; Stewart, J. J. P.; Pople, J. A. *GAUSSIAN 92*; Gaussian: Pittsburgh, PA, 1992. Foresman, J. B., Frisch, Æ. *Exploring Chemistry with Electronic Structure Methods*; Gaussian: Pittsburgh, 1993.

29. Curtiss, L. A., Raghavachari, K., Trucks, G. W., Pople, J. A. *J. Chem. Phys.* 94: 7221-7230, 1991. Curtiss, L. A., Raghavachari, K., Pople, J. A. *J. Chem. Phys.* 98: 1293-1298, 1993.

30. Benson, S.W., *Thermochemical Kinetics*, 2nd ed., Wiley and Sons: New York, 1976. Laidler, K.J., *Chemical Kinetics*, 3rd ed., Harper: New York, 1987.

31. Mallard, W.G., Westley, F., Herron, J.T., Hampson, R.F., *NIST Chemical Kinetics Database, Version 5.0*, U.S. Department of Commerce, Gaithersburg, MD, 1993.

32. Temps, F. and Wagner, H. Gg., *Ber. Bunsenges Phys. Chem.* 88: 415 (1984).

33. Cohen, N., *Intern. J. Chem. Kinet.*, 21: 909-922 (1989).

34. Lane, S. *Vibrations for Windows* (CCL Archive, 1995).

35. Tully, F.P., Droege, A.T., Koszykowski, M.L., and Melius, C.M., *J. Phys. Chem.* 90: 691-698 (1986).

36. Kee, R.J., Warnatz, J. and Miller, J.A. Sandia Report *SAND83-8209*, Sandia National Laboratories, 1988.

37. Garrett, B. C., Truhlar, D. G., Grev, R. S. in *Potential Energy Surfaces and Dynamical Calculations* (Ed., Truhlar, D. G.) Plenum: New York, 1981.

Figure Captions

Figure 1. Arrhenius plot of experimental rate measurements for k_1.

Figure 2. Potential energy diagram for OH addition to CH_3CHO. Adduct stabilization, H-atom elimination, and CH_3 elimination channels are shown. Except for CH_3CHO + OH adduct, energies are taken from ref. 25. Adduct energy based on group additivity calculation for $CH_3CH(OH)_2$ and using a O···H bond dissociation energy of 104.2 kcal mol^{-1}.

Figure 3. HF/6-31G(d) geometry for OH abstraction from the CH_3 group in CH_3CHO. Distances in Å: O_1-C_2, 1.198; C_2-H_3, 1.091; C_2-C_4, 1.481; C_4-H_5, 1.305; C_4-H_6, 1.079; C_4-H_7, 1.080; H_5-O_8, 1.219; O_8-H_9, 0.956. Angles in degrees: O_1-C_2-H_3, 120.6; C_2-C_4-H_3, 116.5; C_2-C_4-H_5, 105.2; C_2-C_4-H_6, 114.1; C_2-C_4-H_7, 115.7; C_4-H_5-O_8, 175.4; H_5-O_8-H_9, 99.9. Frequencies (scaled by 0.893) in cm^{-1}: 2943i, 62, 131, 145, 369, 483, 490, 744, 880, 913, 1048, 1097, 1164, 1378, 1396, 1423, 1583, 2862, 2936, 3017, 3596.

Figure 4. Arrhenius plot of QRRK model results for k_1. k_{1a}: OH addition/CH_3 elimination, k_{1b}: OH addition/H elimination, k_2: H-atom abstraction from ketyl group, k_3: H-atom abstraction from -CH_3 group, k_{tot}: sum of calculated rate coefficients for all channels, k_{exp}: experimental observed rate coefficients. The calculated rate coefficients for stabilization of the OH + CH_3CHO adduct were less than 1×10^{10} cm^3/mol-s and are not shown.

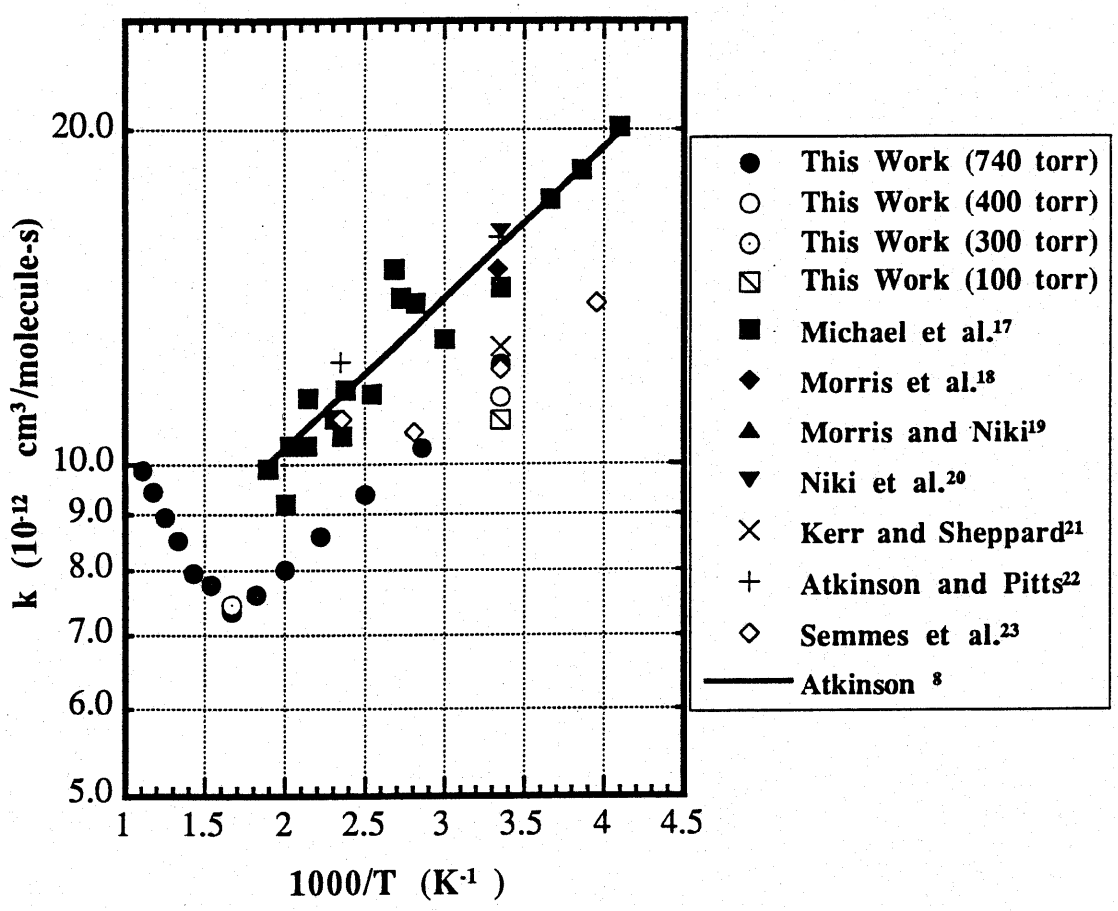

Figure 1. Taylor et al.

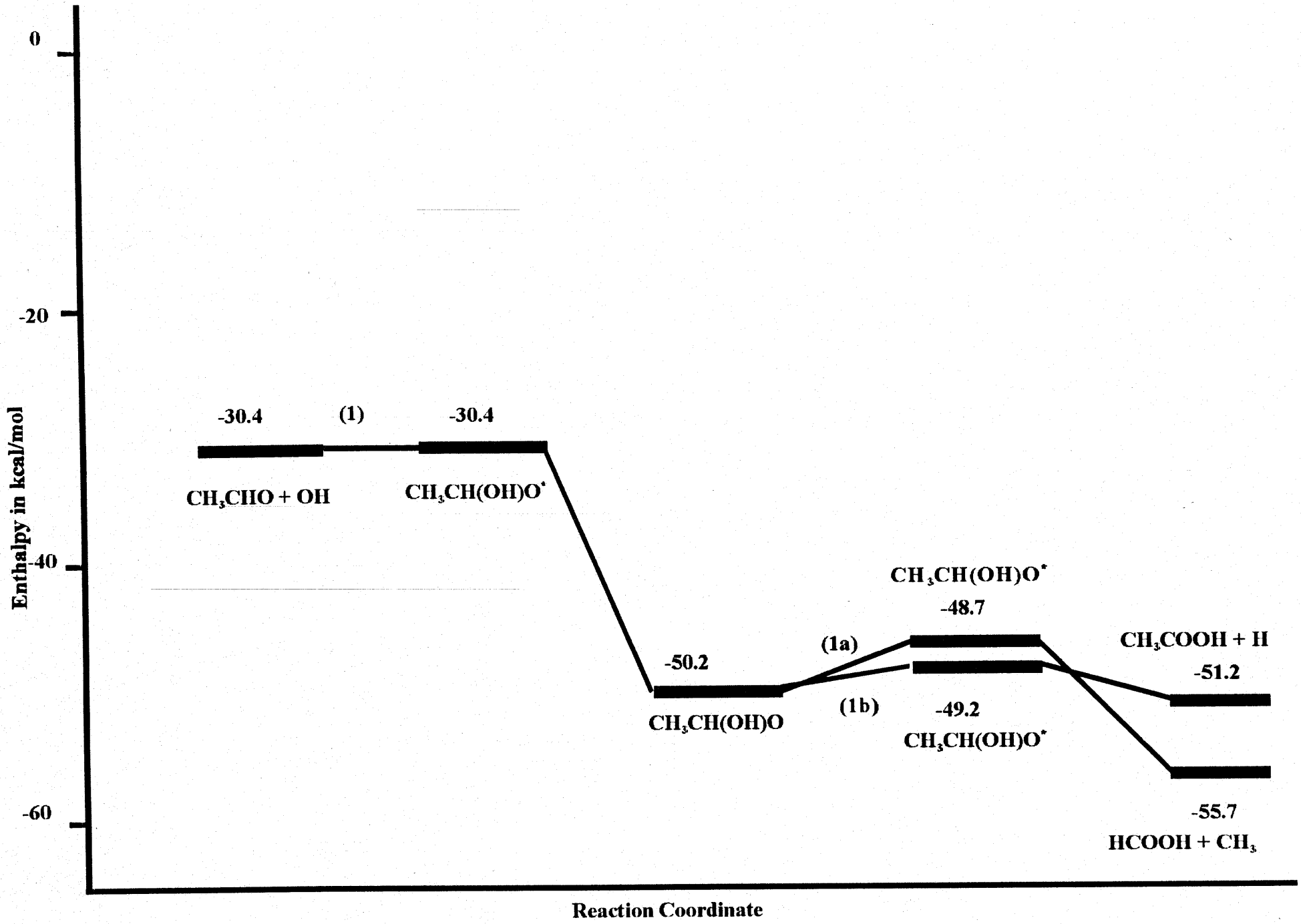

Figure 2. Taylor et al.

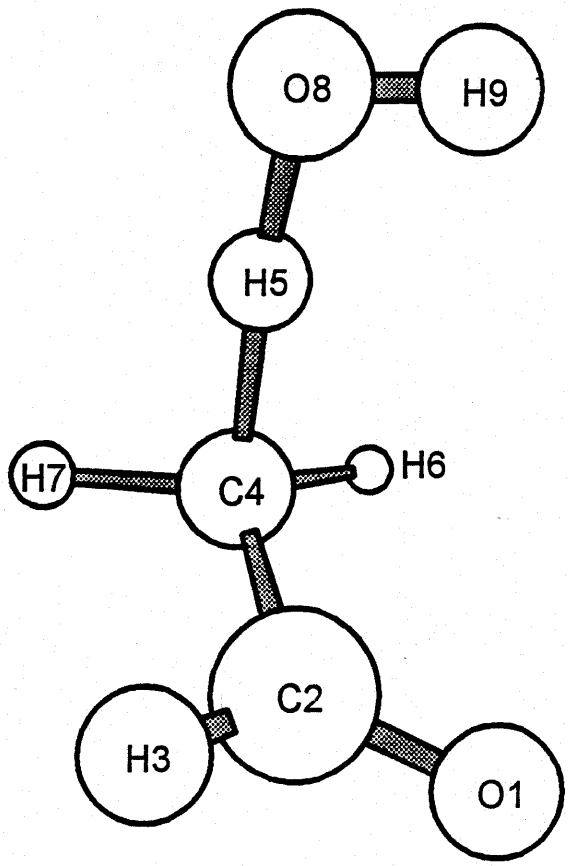

Figure 3. Taylor et al.

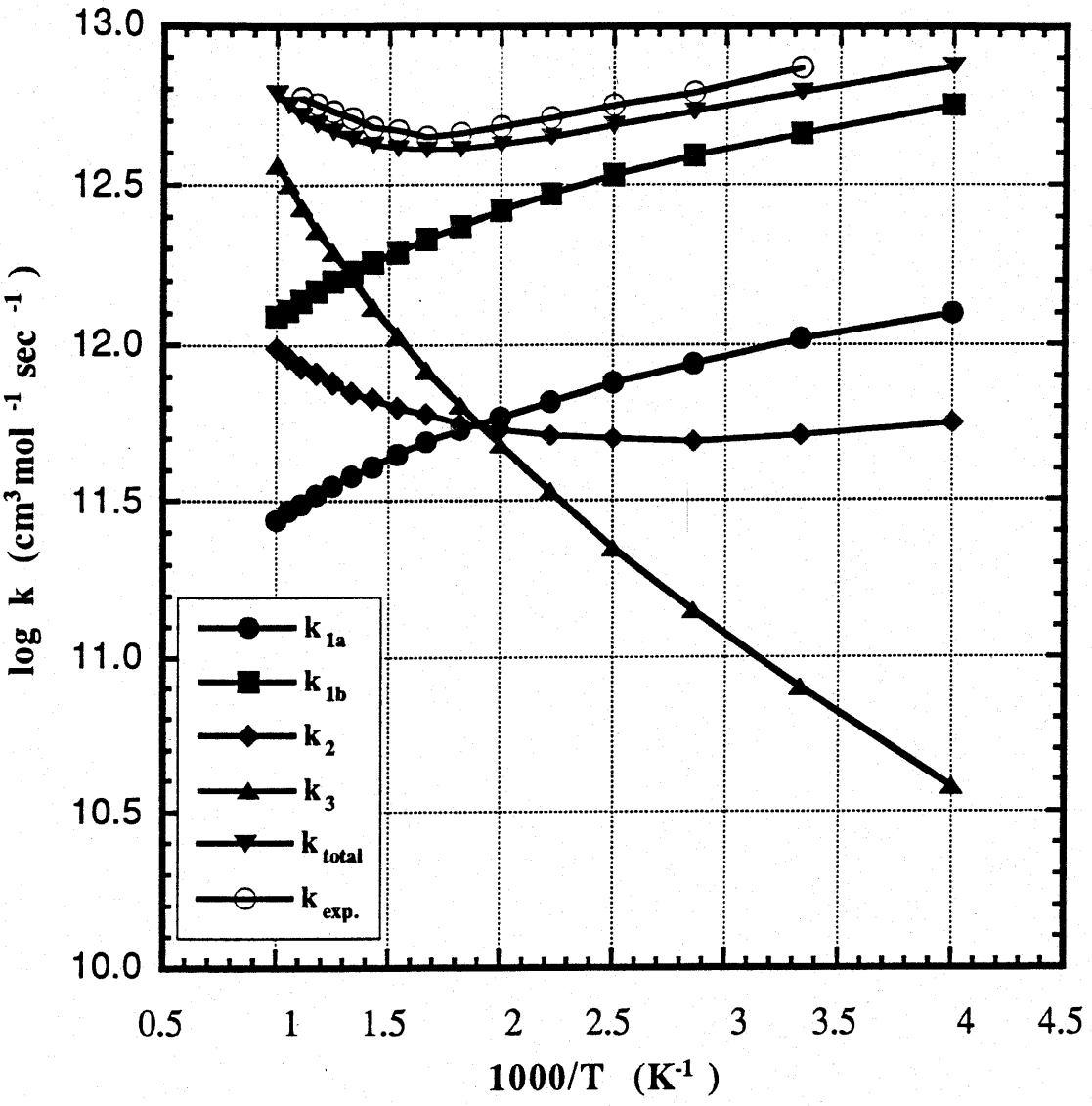

Figure 4. Taylor et al.

Table 1
Input QRRK Parameters

High Pressure Limit Rate Coefficients (units of cm^3-mole-s-cal):

$k_1 = 3.00 \times 10^{15} T^{-1.1}$ (cm^3/mole-s)
$k_{-1} = 3.81 \times 10^{10} \exp(-20{,}220/RT)$ (1/s)
$k_{1a} = 1.10 \times 10^{14} \exp(-1{,}680/RT)$ (1/s)
$k_{1b} = 2.36 \times 10^{13} \exp(-350/RT)$ (1/s)
$k_2 = 2.00 \times 10^{6} T^{1.8} \exp(1{,}300/RT)$ (cm^3/mole-s)
k_3 (free rotation)$= 1.55 \times 10^{6} T^{2.20} \exp(-1{,}000/RT)$ (cm^3/mole-s)
k_3 (hindered rotation)$= 8.92 \times 10^{5} T^{2.57} \exp(-1{,}000/RT)$ (cm^3/mole-s)

Adduct Frequency: $\tilde{\nu} = 906\ cm^{-1}$

# of Oscillators: $s = 21$

Lennard-Jones Parameters:

$CH_3CHO(OH)$ adduct:	$\sigma = 3.360$ Å, $\epsilon/k_B = 186.8$ K.
He bath gas:	$\sigma = 2.576$ Å, $\epsilon/k_B = 470.0$ K.

Table 2
Deuterated Isotope Data[a]

T, K	k_{CH3CHO}	k_{CH3CDO}	k_{CD3CDO}	k_{CH3CHO}/k_{CH3CDO}	k_{CH3CHO}/k_{CD3CDO}
298	1.23×10^{-11}	9.42×10^{-12}	1.02×10^{-11}	1.31	1.21
400	9.38×10^{-12}	8.95×10^{-12}	7.85×10^{-12}	1.05	1.19
600	7.41×10^{-12}	7.35×10^{-12}	6.02×10^{-12}	1.01	1.23
750	8.52×10^{-12}	8.65×10^{-12}	7.28×10^{-12}	0.98	1.17

[a] Units of cm^3 $molecule^{-1}$ s^{-1}.